J|A|C|S
ARTICLES
Published on Web 11/15/2002

Side Chain Orientation from Methyl ^{1}H−^{1}H Residual Dipolar Couplings Measured in Highly Deuterated Proteins

Nathalie Sibille,[†] Beate Bersch,[†] Jacques Covès,[‡] Martin Blackledge,[†] and Bernhard Brutscher*,[†]

Contribution from the Institut de Biologie Structurale, Jean-Pierre Ebel C.N.R.S.-C.E.A., 41 rue Jules Horowitz, 38027 Grenoble Cedex, France and Laboratoire de Chimie et Biochimie des Centres Rédox Biologiques, CEA-Grenoble, UMR 5047 CNRS-CEA-UJF, 17 Avenue des Martyrs, 38054 Grenoble Cedex 9, France

Received June 27, 2002

Abstract: High-level deuteration is a prerequisite for the study of high molecular weight systems using liquid-state NMR. Here, we present new experiments for the measurement of proton−proton dipolar couplings in CH_2D methyl groups of ^{13}C labeled, highly deuterated (70−80%) proteins. ^{1}H−^{1}H residual dipolar couplings (RDCs) have been measured in two alignment media for 57 out of 70 possible methyl containing residues in the 167-residue flavodoxin-like domain of the *E. coli* sulfite reductase. These data yield information on the orientation of the methyl symmetry axis with respect to the molecular alignment frame. The alignment tensor characteristics were obtained very accurately from a set of backbone RDCs measured on the same protein sample. To demonstrate that accurate structural information is obtained from these data, the measured methyl RDCs for Valine residues are analyzed in terms of χ_1 torsion angles and stereospecific assignment of the prochiral methyl groups. On the basis of the previously determined backbone solution structure of this protein, the methyl RDC data proved sufficient to determine the χ_1 torsion angles in seven out of nine valines, assuming a single-rotamer model. Methyl RDCs are complementary to other NMR data, for example, methyl−methyl NOE, to determine side chain conformation in high molecular weight systems.

Introduction

Residual dipolar couplings (RDCs) measured for weakly aligned proteins provide important structural restraints for molecular fold determination by liquid-state NMR.[1] With the introduction of numerous alignment media,[2−4] RDC measurements have become widely used in the biomolecular NMR community. RDC measurements are generally performed on highly deuterated protein samples to avoid extensive line broadening of ^{1}H resonances due to ^{1}H−^{1}H RDC. A protonation level of 70−80% is routinely obtained by protein overexpression in *E. coli* using a minimal medium containing D_2O (>90%) and [U-^{13}C,^{1}H]glucose. Recent applications have focused on the use of backbone RDC to define the relative orientation of molecular domains,[5] to validate structural homology models[6] or to improve the accuracy of structures determined by NMR.[7] It has also been shown that an accurate three-dimensional model of the protein backbone can be built *de novo* from RDC data alone.[8] Despite the intense activity centered around the measurement and interpretation of backbone RDC, relatively few RDC measurements have so far been reported for protein side chains.[9−13] Methyl containing side chains are of special interest

* Correspondence to be addressed to Dr. Bernhard Brutscher, Laboratoire de RMN, Institut de Biologie Structurale, Jean-Pierre Ebel, 41 rue Jules Horowitz, 38027 Grenoble Cedex 1, France. E-mail: Bernhard.Brutscher@ibs.fr.

[†] Institut de Biologie Structurale, Jean-Pierre Ebel.

[‡] Laboratoire de Chimie et Biochimie des Centres Rédox Biologiques.

(1) Bax, A.; Kontaxis, G.; Tjandra, N. *Methods Enzymol.* **2001**, *339*, 127−174.

(2) Ottiger, M.; Bax, A. *J. Biomol. NMR* **1998**, *12*, 361−372. Wang, H.; Eberstadt, M.; Olejniczak, E. T.; Meadows, R. P.; Fesik, S. W. *J. Biomol. NMR* **1998**, *12*, 443−446. Clore, G. M.; Starich, M. R.; Gronenborn, A. M. *J. Am. Chem. Soc*. **1998**, *120*, 10571−10572. Saas, J.; Cordier, F.; Hoffmann, A.; Rogowski, M.; Cousin, A.; Omichinski, J. G.; Löwen, H.; Grzesiek, S. *J. Am. Chem. Soc*. **1999**, *121*, 2047−2055. Tycko, R.; Blanco, F. J.; Ishii, Y. *J. Am. Chem. Soc*. **2000**, *122*, 9340−9341. Flemming, K.; Gray, D.; Prasannan, S.; Matthews, S. *J. Am. Chem. Soc*. **2000**, *122*, 5224−5225.

(3) Hansen, M. R.; Mueller, L.; Pardi, A. *Nat. Struct. Biol*. **1998**, *5*, 1065−1074.

(4) Rückert, M.; Otting, G. *J. Am. Chem. Soc*. **2000**, *122*, 7793−7797.

(5) Fischer, M. W. F.; Losonczi, J. A.; Weaver, J. L.; Prestegard, J. H. *Biochemistry* **1999**, *38*, 9013−9022. Skrynnikov, N. R.; Goto, N. K.; Yang, D.; Choy, W.-Y.; Tolman, J. R.; Mueller, G. A.; Kay, L. E. *J. Mol. Biol*. **2000**, *295*, 1265−1273.

(6) Annila, A.; Aito, H.; Thulin, E.; Drakenberg, T. *J. Biomol. NMR* **1999**, *14*, 223−230. Meiler, J.; Peti, W.; Griesinger, C. *J. Biomol. NMR* **2000**, 17, 283−294. Chou, J. J.; Li, S.; Bax, A. *J. Biomol. NMR* **2000**, *18*, 217−227.

(7) Tjandra, N.; Omichinski, J. G.; Gronenborn, A. M.; Clore, G. M.; Bax, A. *Nature Struct. Biol*. **1997**, *4*, 732−738. Clore, G. M.; Starich, M. R.; Bewley, C. A.; Cai, M.; Kuszewski, J. *J. Am. Chem. Soc*. **1999**, *121*, 6513−6514. Mueller, G. A.; Choy, W. Y.; Skrynnikov, N. R.; Kay, L. E. *J. Biomol. NMR* **2000**, *18*, 183−188.

(8) Delaglio, F.; Kontaxis, G.; Bax, A. *J. Am. Chem. Soc*. **2000**, *122*, 2142−2143. Hus, J. C.; Marion, D.; Blackledge, M. *J. Am. Chem. Soc*. **2001**, *123*, 1541−1542.

(9) Ottiger, M.; Delaglio, F.; Marquardt, J. L.; Tjandra, N.; Bax, A. *J. Magn. Reson*. **1998**, *134*, 365−369. Carlomagno, T.; Peti, W.; Griesinger, C. *J. Biomol. NMR* **2000**, *17*, 99−109. Evenäs, J.; Mittermaier, A.; Yang, D.; Kay, L. E. *J. Am. Chem. Soc*. **2001**, *123*, 2858−2864. Chou, J. J.; Bax, A. *J. Am. Chem. Soc*. **2001**, *123*, 3844−3845.

(10) Kaikkonen, A.; Otting, G. *J. Am. Chem. Soc*. **2001**, *123*, 1770−1771.

(11) Kontaxis, G.; Bax, A. *J. Biomol. NMR* **2001**, *20*, 77−82.

(12) Olejniczak, E. T.; Meadows, R. P.; Wang, H.; Cai, M.; Hettesheim, D. G.; Fesik, S. W. *J. Am. Chem. Soc*. **1999**, *121*, 9249−9250.

10.1021/ja020888m CCC: $22.00

for structure determination, as they are often found in the hydrophobic core or active sites of proteins. Here, we show that $^1H-^1H$ methyl RDC can be measured accurately using the same highly deuterated and weakly aligned protein sample as used for the measurement of backbone RDC such that the measured backbone and methyl RDC provide geometric information with respect to the same molecular alignment frame.

Because of the rapid rotation of the methyl protons around their 3-fold symmetry axis, the $^1H-^1H$ or $^1H-^{13}C$ RDC measured for spin pairs within the methyl group reflect the orientation of the C_3 symmetry axis with respect to the alignment tensor. For structure calculation purposes, the RDC values are thus most easily converted into a restraint for the preceding C−C bond orientation. Although the rapid methyl rotation reduces the dipolar coupling compared to the static case, $^1H-^1H$ and $^1H-^{13}C$ RDC values for a given methyl group are still about 7 and 3 times larger than the corresponding $^{13}C-^{13}C$ RDC. Several experiments have been proposed in the past to measure $^1H-^{13}C$ couplings of methyl groups. These include the recording of a 2D $^1H-^{13}C$ HSQC or 3D HCCH type correlation spectrum that is ^{13}C coupled in the ^1H dimension[12] or the recording of a set of J_{CH}-modulated CT-HSQC type experiments.[14] It has also been proposed to use multiplet component separation to simplify the ^{13}C spectra of CH_3 groups recorded in the absence of ^1H decoupling.[11] The RDC is then obtained from the difference in the coupling constant measured in anisotropic and isotropic solution. A method to measure $^1H-^1H$ RDC has recently been proposed by Kaikkonen and Otting.[10] In their experiment, the D_{HH}^{met} coupling is manifest as an antiphase splitting in the ^1H dimension of a $^1H-^{13}C$ correlation experiment. For the measurement of D_{HH}^{met} coupling constants, no reference experiment is required, as the scalar contribution to the measured spin−spin coupling in methyl groups is zero. All the earlier-described experiments were designed for application to fully protonated CH_3 groups.

In this paper, we propose new experiments for the measurement of the sign and magnitude of D_{HH}^{met} RDC in highly deuterated protein samples. A 2D constant time (CT) HSQC experiment yields sufficient resolution for small to medium size proteins with a sufficiently well resolved $^1H-^{13}C$ correlation spectrum for the methyl region. For larger systems, a 3D double CT-HCC experiment is required to resolve overlapping methyl $^1H-^{13}C$ correlation peaks by the resonance frequency of the directly attached carbon. The additional $^{13}C-^{13}C$ coherence transfer is highly efficient because of the particular position of the methyl groups at the side chain ends and the favorable relaxation properties of the methyl ^{13}C. In both experiments, the CH_2D isotopomers are selected by means of specific pulse sequence elements. The D_{HH}^{met} coupling is obtained from the doublet splitting in the ^1H dimension. The two doublet lines are separated in different spectra by a spin-state-selection filter.[15,16] The experiments are demonstrated on a uniformly ^{13}C, ^{15}N, and 77% ^2H labeled sample of the flavodoxin-like domain of the *E. coli* sulfite reductase (SiR-FP18), a globular protein of 167 amino acids.[17] RDCs are measured for two different alignment media: a Pf1 phage[3] and an alkyl poly(ethylene glycol) mixture.[4] The standard procedure for interpreting RDC is to insert a penalty function into a molecular-dynamics-based structure calculation protocol. While it is possible to interpret D_{HH}^{met} to refine the methyl containing side chain orientations in this way, in this communication we present an algorithm to simultaneously determine χ_1 torsion angles as well as stereospecific assignment of the two prochiral methyl groups in valine side chains. This algorithm is compatible with the program MODULE[18] and is available free of charge from the authors.

Experimental Section

NMR Samples of SiR-FP18. ^{13}C, ^{15}N, and ^2H labeled SiR-FP18, corresponding to residues 52−218 of the *E. coli* sulfite reductase flavoprotein component was prepared as described elsewhere.[17,19] The deuteration level was 77%, as deduced from mass spectroscopy. After purification, the protein was reconstituted with commercial FMN (Sigma). All NMR samples were prepared in a 100 mM potassium phosphate buffer at pH 7.0 containing 0.02% sodium azide at a protein concentration of about 1.5 mM. A first sample in isotropic solution was used for assignment of the methyl ^1H and ^{13}C resonances. Two aqueous liquid-crystalline NMR samples were prepared. For the phage sample, SiR-FP18 was suspended in a solution consisting of 14 mg/mL of filamentous Pf1 phage (Asla Ltd, Riga, Latvia) and for the alcohol sample, SiR-FP18 was dissolved in a solution consisting of 5% C12E5/hexanol with $r = 0.96$.[4]

NMR Data Acquisition and Processing. NMR experiments were performed on a VARIAN 600 MHz spectrometer, equipped with a triple-resonance (^1H, ^{13}C, ^{15}N) probe and shielded pulsed-field gradients along the *z*-axis. All data sets were recorded at a sample temperature of 30 °C. Data processing and determination of peak positions were performed using FELIX program version 2000 (Accelrys Inc.).

RDC Measurements. For the 2D D_{HH}-CT-HSQC experiments, data sets of 140($^{13}C^1$) × 512(^1H) complex points were recorded for spectral widths of 5000 Hz ($^{13}C^1$) and 8000 Hz (^1H) in an experimental time of 10 h. 3D data sets of the D_{HH}-CT-HCC experiment were acquired with 57($^{13}C^1$) × 60($^{13}C^2$) × 512(^1H) complex points for spectral widths of 4000 Hz ($^{13}C^1$), 5000 Hz ($^{13}C^2$), and 8000 Hz (^1H) in an experimental time of 70 h. Mirror-image linear prediction[20] was applied to the ^{13}C CT dimensions of the 2D and 3D data sets. Squared cosine apodization was used in all dimensions, prior to zero-filling and Fourier transformation. The D_{HH}^{met} coupling constants were obtained from the relative peak positions in the ^1H dimension measured in the α and β subspectra.

Additional 2D $^1H-^{15}N$ α/β HSQC spectra were recorded for both liquid-crystalline samples with 128 (^{15}N) × 512(^1H) complex points and spectral widths of 1800 Hz (^{15}N) and 9000 Hz (^1H) in an experimental time of 10 h. $J_{NH} + D_{NH}$ coupling constants were obtained from these spectra from the relative peak positions in the ^{15}N dimension measured in the α and β subspectra.

Side Chain Resonance Assignment. The ^1H and ^{13}C resonance frequencies of the aliphatic side chains were previously assigned from a set of ^{13}C TOCSY experiments recorded on a fully protonated sample of SiR-FP18.[19] In the present context, it is useful to demonstrate that methyl resonance assignment is also obtained from spectra recorded on a 77% deuterated sample. Therefore, 3D (H)C(CO)NH-TOCSY and H(CCO)NH-TOCSY spectra[21] were recorded on the triple labeled (^{13}C,

(13) Mittermaier, A.; Kay, L. E. *J. Am. Chem. Soc*. **2001**, *123*, 6892−6903.
(14) Tjandra, N.; Bax, A. *J. Magn. Reson*. **1997**, *124*, 512−515.
(15) Meissner, A.; Duus, J. Ø.; Sørensen, O. W. *J. Magn. Reson*. **1997**, *128*, 92−97. Ottiger, M.; Delaglio, F.; Bax, A. *J. Magn. Reson*. **1998**, *131*, 373−378. Anderson, P.; Weigelt, J.; Otting, G. *J. Biomol. NMR* **1998**, *12*, 435−441.
(16) Brutscher, B. *J. Magn. Reson*. **2001**, *51*, 332−338.
(17) Champier, L.; Sibille, N.; Bersch, B.; Brutscher, B.; Blackledge, M.; Covès, J. *Biochemistry* **2002**, *41*, 3770−3780.
(18) Dosset, P.; Hus, J.-C.; Marion, D.; Blackledge, M. *J. Biomol. NMR* **2001**, *20*, 223−231.
(19) Sibille, N.; Covès, J.; Marion, D.; Brutscher, B.; Bersch, B. *J. Biomol. NMR* **2001**, *21*, 71−72.
(20) Zhu, G.; Bax, A. *J. Magn. Reson*. **1990**, *90*, 405−410.
(21) Grzesiek, S.; Anglister, J.; Bax, A. *J. Magn. Reson., Ser. B* **1993**, *101*, 114−119.

^{15}N, 77% ^{2}H) SiR-FP18 sample in isotropic solution. The same sample was previously used for sequential backbone resonance assignment.[19] The high quality of the obtained spectra is shown in Figure S2 of the Supporting Information. Complete resonance assignment of the methyl ^{1}H and ^{13}C was obtained from these spectra for all residues except those preceding prolines. The assignment was completed from additional (H)CNH-TOCSY and H(C)NH-TOCSY spectra recorded on the same sample. In the case of overlapping ^{1}H−^{13}C correlation peaks, they are separated in the 3D CT-HCC spectra by the amino acid type characteristic C^2 frequency. The C^α frequency of alanine and C^β frequencies of threonine, valine, and isoleucine are generally known from the backbone resonance assignment. The unassigned $C^{\gamma 1}$ of isoleucine and C^γ of leucine can be distinguished in the CT-HCC spectrum by their different signs due to a pair and impair number of attached ^{13}C, respectively.

Data Analysis. The alignment tensor parameters (the axial and rhombic components, A_a and A_r, and Euler angles $\{\alpha, \beta, \gamma\}$) define the nonaveraged orientation of the molecule relative to an external reference frame. These five parameters were determined by nonlinear least-squares minimization of the target function using the program MODULE.[18] The two alignment tensors were characterized using D_{NH-N}, $D_{C\alpha-C'}$, and $D_{NH-C'}$ dipolar couplings in comparison with the three-dimensional coordinates of the previously modeled structure, derived from primary sequence alignment and the program Swiss-Model.[22] Only RDCs measured in secondary structural elements were used for this analysis.[17]

The model structure was then refined so that the backbone was in best agreement with the two sets of data. This was achieved using the restrained molecular dynamics program SCULPTOR[23] in the presence of restraints derived from backbone residual dipolar couplings (D_{NH-N}, $D_{C\alpha-C'}$, $D_{NH-C'}$) measured in both alignment media. As in our previous study using one set of RDCs, a tethering potential was applied to the C_α atoms of the peptide chain in order to avoid simple expansion of the molecular model.[17] Additional restraints included backbone dihedral angle restraints derived from CSI values in the secondary structural elements and hydrogen bonds identified from the direct measurement via scalar coupling constants. The tensor eigenvalues (defined by the values of A_a and A_r) were fixed at the values determined using MODULE, and the orientation of the alignment tensors was allowed to evolve freely during the calculation. The system was equilibrated at 300 K for 0.5 ps of molecular dynamics and gradually increased to 500 K over a period of 2 ps, during which period k_{RDC} was increased from 0.1 to 1.0 kcal mol^{-1} Hz^{-2}. A total of 5000 steps of sampling at 500 K was followed by slow cooling to 100 K. The lowest target function structure was used for further analysis of the methyl side chain conformation.

An algorithm was developed to determine the χ_1 conformation from measured D_{HH}^{met} and the known conformation of the C−C vector preceding the methyl group containing carbon. In the case of valine, this is the C^α−C^β bond, whose orientation is defined in the structure refined using two sets of backbone RDC. The algorithm requires the coordinates of the two carbon atoms, the atom preceding the initial carbon in the primary sequence (the amide nitrogen of the same residue in the case of valine), and the five parameters defining each of the two alignment tensors. For the sake of simplicity, the calculation is performed in the frame of the input coordinates (normally the pdb frame) and the coordinate rotations. Euler angles and tensor eigenvalues are compatible with the program MODULE. These parameters are then used to calculate the arc of potential C_γ positions, and the values of D_{HH}^{met} for both the $C^{\gamma 1}$ and $C^{\gamma 2}$ sites are determined for the whole range of χ_1, in the presence of both alignment tensors. A total target function taking into account all four RDCs measured at a given χ_1 is then calculated for each of the possible stereospecific assignments. For side chains containing only one methyl group attached to the C_β (isoleucine, threonine), a simpler procedure is applied with no stereospecific information.

Theoretical Background

Assuming the global shape of the molecule is constant, we can express the measured residual dipolar coupling D_{IS} between two nuclear spins I and S in terms of the orientation $\{\theta, \phi\}$ of the internuclear vector relative to the common alignment tensor of the molecule in anisotropic solution:

$$D_{IS} = SD_{IS}^{max}\left[\frac{1}{2}A_a(3\cos^2\theta - 1) + \frac{3}{2}A_r\sin^2\theta\cos(2\phi)\right] \quad (1)$$

where A_a and A_r are the axial and rhombic components of the alignment tensor and S is a generalized order parameter taking into account local motion of the I−S vector on a pico- to millisecond time scale.[24] D_{IS}^{max} is the static dipolar coupling measured for an I−S vector oriented parallel to the magnetic field given by

$$D_{IS}^{max} = -\frac{\mu_0}{4\pi^2}\gamma_I\gamma_S\hbar\langle r_{I-S}^{-3}\rangle \quad (2)$$

where the brackets around r_{I-S}^{-3} account for vibrational averaging of the internuclear distance r_{I-S}. For practical applications, it is convenient to use an experimentally determined effective bond length[25] defined as

$$(r_{I-S}^{eff})^{-3} = \langle r_{I-S}^{-3}\rangle \quad (3)$$

For the ^{1}H−^{13}C dipolar coupling in methyl groups, the rapid rotation around the C_3 symmetry axis can be taken into account by an order parameter $S^{rot} = (3\cos^2\beta - 1)/2$ where β is the angle between the methyl C−H bond and the symmetry axis. This is valid independently of whether the methyl group rotates freely about the C_3 axis or executes equally probable three-site jumps about this axis.[26]

$$D_{HH}^{met} = S^*\frac{3\cos^2\beta - 1}{2}D_{HH}^{max}\left[\frac{1}{2}A_a(3\cos^2\theta_S - 1) + \frac{3}{2}A_r\sin^2\theta_S\cos(2\phi_S)\right] \quad (4)$$

The new order parameter S^* represents averaging from motional modes other than the methyl rotation. An analogous expression for the D_{HH}^{met} coupling in methyls has been derived recently by Kaikkonen and Otting[10] on the basis of symmetry considerations of the spin Hamiltonian. They show that the methyl rotation reduces the ^{1}H−^{1}H dipolar coupling by a factor of $-3/4$ with respect to the static case.

$$D_{HH}^{met} = -\frac{3}{4}S^*D_{HH}^{max}\left[\frac{1}{2}A_a(3\cos^2\theta_S - 1) + \frac{3}{2}A_r\sin^2\theta_S\cos(2\phi_S)\right] \quad (5)$$

The angles $\{\theta_S, \phi_S\}$ in eqs 4 and 5 describe the orientation of

(22) Guex, N.; Peitsch, M. C. *Electrophoresis* **1997**, *18*, 2714−2723.
(23) Hus, J. C.; Marion, D.; Blackledge, M. *J. Mol. Biol.* **2000**, *298*, 927−936.
(24) Lipari, G.; Szabo, A. *J. Am. Chem. Soc.* **1982**, *104*, 4546−4559. Lipari, G.; Szabo, A. *J. Am. Chem. Soc.* **1982**, *104*, 4559−4570. Peti, W.; Meiler, J.; Brüschweiler, R.; Griesinger, C. *J. Am. Chem. Soc.* **2002**, *124*, 5822−5833.
(25) Ottiger, M.; Bax, A. *J. Am. Chem. Soc.* **1998**, *120*, 12334−12341.
(26) Mittermaier, A.; Kay, L. E. *J. Am. Chem. Soc.* **1999**, *121*, 10608−10613.

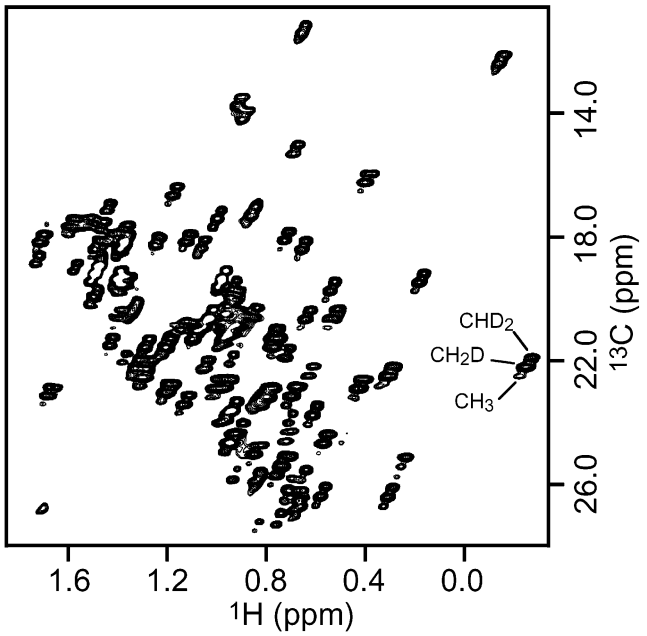

Figure 1. Methyl region of a $^1H-^{13}C$ CT-HSQC spectrum of SiR-FP18 in isotropic solution recorded at 30°C and 600 MHz ^1H frequency. For each methyl, three correlation peaks are detected corresponding to the CH_2D, CHD_2, and CH_3 isotopomers. The intensity distribution of the three peaks is characteristic of a highly deuterated protein sample.

the C_3 symmetry axis relative to the molecular alignment frame. For a given methyl group, the ratio of the two couplings becomes independent of the alignment tensor, the internuclear distances, and the local order parameter S^* and provides a measure of the methyl geometry via the projection angle β:

$$\lambda_1 = \frac{D_{HH}^{met}}{D_{CH}^{met}} = -\frac{3}{2}\frac{\gamma_H}{\gamma_C}(3\cos^2\beta - 1)^{-1}(2\sin(\pi/3)\sin\beta)^{-3} \quad (6)$$

For ideal tetrahedral geometry $\beta = 109.5°$, this ratio becomes $\lambda_1 \cong 2.06$. Recent NMR work of Ottinger and Bax on fully protonated methyl groups in proteins[27] indicates an average value of $\beta = 110.9°$, which results in a slightly (10%) higher ratio of $\lambda_1 \cong 2.28$.

A measured D_{HH}^{met} coupling can be used as constraint for the C^1-C^2 bond vector orientation using the relation:

$$D_{HH}^{met} = \lambda S^* D_{CC}^{max}\left[\frac{1}{2}A_a(3\cos^2\theta_S - 1) + \frac{3}{2}A_r\sin^2\theta_S\cos(2\phi_S)\right] \quad (7)$$

with $\lambda = \lambda_1\lambda_2\lambda_{scale}$. λ_1 is the ratio defined in eq 6. The conversion factor $\lambda_2 = D_{CH}^{met}/D_{CC}$, which depends on the methyl geometry and the effective C−H and C−C bond lengths, has been determined experimentally to be $\lambda_2 = -3.17$.[27] λ_{scale} is a scaling factor taking into account eventual changes in the alignment tensors principal axes components over time (see later).

Results and Discussion

Measurement of $^1H-^1H$ Dipolar Couplings in Methyl Groups. Figure 1 shows the methyl region of a standard $^1H-^{13}C$ CT-HSQC spectrum recorded on a ^{13}C, ^{15}N, and 77% ^2H labeled SiR-FP18 sample in isotropic solution. The methyl resonance frequencies were assigned from a set of amide proton detected ^{13}C-TOCSY experiments,[21] recorded on the same sample (see Figure S2 of the Supporting Information). For each methyl site, three correlation peaks can be distinguished corresponding to the CHD_2, CH_2D, and CH_3 isotopomers, separated by the characteristic deuterium isotope shifts. Experimentally, we find relative average peak intensities of roughly 50% (CHD_2), 40% (CH_2D), and 10% (CH_3), which is close to the intensity distribution expected for a 77% randomly deuterated sample. Thus, experimental methods for the measurement of residual dipolar couplings in either CHD_2 or CH_2D methyl groups should be applicable to proteins with a level of deuteration as high as 77%. Here, we focus on D_{HH}^{met} dipolar couplings in CH_2D methyl groups, which presents some major advantages over alternative methods: (i) the CH_2D isotopomers can be selected properly even for partially aligned molecules in anisotropic solution, (ii) the range of D_{HH}^{met} coupling constants for a given molecular alignment is about two times larger than that for D_{CH}^{met} couplings (see eq 6), and (iii) the RDC values are obtained from a single experiment recorded on a sample dissolved in a liquid-crystalline medium. No reference experiment is needed because of the absence of a scalar coupling contribution to the ^1H line splitting.

2D D_{HH}-CT-HSQC Method. Measurement of $^1H-^1H$ residual dipolar couplings in CH_2D methyl groups is achieved by using the pulse sequence of Figure 2A. The experiment is derived from a standard CT-HSQC experiment by adding two additional features: (i) a CH_2D isotopomer selection filter and (ii) an α/β spin-state selection filter. Both filters exploit the large one-bond $^1H-^{13}C$ coupling for selection.

For isotopomer selection, the different time dependences of the antiphase coherence $2C_yH_z$ on the $^1H-^{13}C$ coupling evolution during a constant time delay 2Δ is exploited:

$$2C_yH_z \rightarrow 2C_yH_z\cos^n(\pi J_{CH}^{eff}2\Delta) \quad (8)$$

$J_{CH}^{eff} = J_{CH} + D_{CH}$ is the effective coupling constant, and n the number of ^1H attached to a methyl ^{13}C. In the two-step version of the filter, two experiments are recorded with delay settings (a) $\Delta = 0$ and (b) $\Delta = 1/2J_{CH}$. The filter can be realized during the CT ^{13}C frequency-editing period (between time points b and c) by adjusting the position of the 180° ^1H inversion pulse. This ensures equal relaxation-induced signal loss for the two experiments. For samples in isotropic solution, the filter delay Δ can be accurately adjusted to the average scalar coupling value in methyls ($J_{CH} \cong 128$Hz), and addition of the two experiments yields almost perfect suppression of the unwanted signals from CHD_2 and CH_3 moieties. In an anisotropic medium, however, the effective $^{13}C-^1H$ coupling constant becomes orientation dependent because of the presence of the dipolar contribution D_{CH}. The filter efficiency defined as the intensity ratio of the suppressed and selected peaks, I^{sup}/I^{sel}, becomes a function of the J mismatch, $J_{CH}^{mis} = |D_{CH}/J_{CH}|$. The filter efficiency of the two-step filter for CHD_2 suppression is drawn in Figure 3A as a function of J^{mis}. Using a concept similar to the recently introduced DIPSAP filter for α/β spin-state selection,[16] the performance of the isotopomer selection can be further increased by performing a third experiment with the delay setting (c) $\Delta = 1/J_{CH}$. The linear combination $ka + b + (1 - k)c$ with $k = 0.75$ yields J mismatch compensation up to third order. For

(27) Ottiger, M.; Bax, A. *J. Am. Chem. Soc.* **1999**, *121*, 4690−4695.

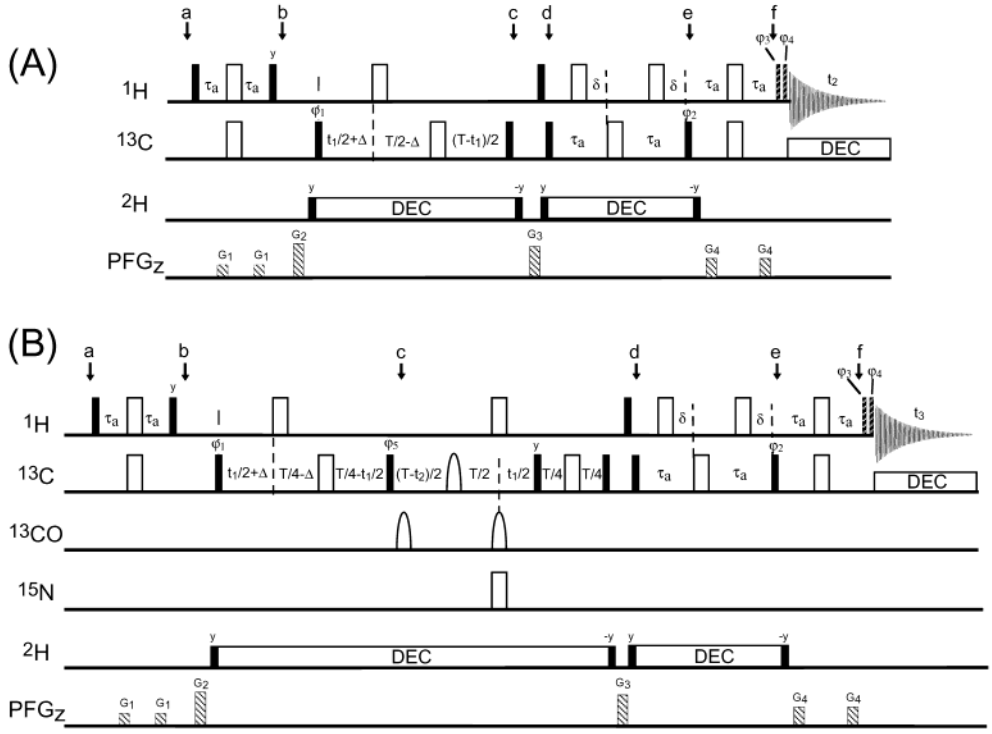

Figure 2. Pulse sequences for (A) 2D D_{HH}-CT-HSQC and (B) 3D D_{HH}-CT-HCC experiments to measure $^1H-^1H$ dipolar couplings in CH_2D methyl groups of highly deuterated ^{13}C and ^{15}N labeled proteins. All radio frequency (rf) pulses are applied along the *x* axis unless indicated. 90° and 180° rf pulses are represented by filled and open pulse symbols, respectively. The dashed narrow pulses at point f are applied with a flip angle of 45°. (B) The shaped refocusing ^{13}C pulse applied during the CT-t_2 period has a BURP profile (400 μs at 150 MHz), and the ^{13}CO 180° pulses have the shape of the center lobe of a sin *x*/*x* function (80 μs). The ^1H, ^{13}C, ^{15}N, and ^2H carriers are positioned at the water resonance, 35 ppm, 118 ppm, and 3 ppm, respectively. For the ^{13}CO pulses, the ^{13}C carrier is shifted by time-proportional phase incrementation during the pulse to 175 ppm. ^2H decoupling is achieved using a WALTZ pulse train of approximately 1 kHz field strength. Pulsed field gradients, G_1, G_2, G_3, and G_4, are applied along the *z* axis (PFG_z) with a gradient strength of approximately 20 G/cm and lengths ranging from 100 to 500 μs, followed by a recovery delay of 100 μs. The delays are set to $\tau_a = 1/4J_{CH}^{met} \cong 1.9$ ms and $T = 1/J_{CC} \cong 28$ ms; the filter delays Δ and δ are varied between experiments. The phases φ_1 and φ_5 are initially set to $\varphi_1 = x$ and $\varphi_5 = y$. For α/β spin-state selection, two experiments (I) and (II) are recorded with the following delay and phase settings: (I) $\delta = \tau_a/2$, $\varphi_2 = x, x, -x, -x$, $\varphi_3 = x$, $\varphi_4 = x, -x$ and $\varphi_{rec} = x, x, -x, -x$; (II) $\delta = 0$, $\varphi_2 = y, y, -y, -y$, $\varphi_3 = y$, $\varphi_4 = y, -y$ and $\varphi_{rec} = x, -x, -x, x$. Both experiments are repeated three times for *J*-mismatch compensated CH_2D isotopomer selection using the delay settings: (a) $\Delta = 0$, (b) $\Delta = 1/2J_{CH}$, and (c) $\Delta = 1/J_{CH}$. The β subspectrum is obtained by linear combination of the six experiments, 0.73 × (Ia − IIa) + (Ib − IIb) + 0.23 × (Ic − IIc), and the β subspectrum is given by 0.73 × (Ia + IIa) + (Ib + IIb) + 0.23 × (Ic + IIc). For the 3D experiment, it is more convenient to use the two-step filter version for CH_2D selection (see text) which reduces the number of transients to be recorded per (t_1,t_2) increment from 24 to 16. For this case, the α and β subspectra are reconstructed as (Ia − IIa + Ib − IIb) and (Ia + IIa + Ib + IIb), respectively. Quadrature detection in the t_1 (and t_2) dimension is achieved by incrementing the phases φ_1 (φ_1 and φ_5) according to the STATES-TPPI method.

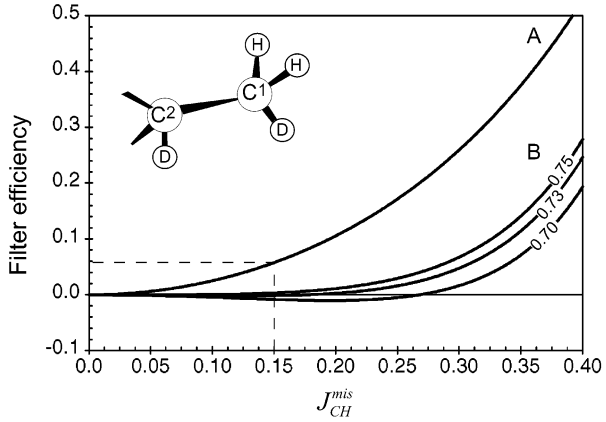

Figure 3. *J*-mismatch profiles calculated for different CH_2D selection filters as discussed in the text: (A) a basic two-step filter and (B) a three-step filter using different scaling factors ranging from $k = 0.70$ to $k = 0.75$.

practical applications, a slightly reduced *k* value should be used to account for the effective range of *J* mismatch. The filter efficiency profile of the three-step filter is plotted in Figure 3B for different values of *k*. The range of *J* mismatch can be estimated from the measured backbone RDC. Bax and coworkers[1] report a value of 0.628 for the magnitude of D_{CH}^{met} relative to the backbone D_{NH}. For the case of partial molecular alignment yielding $|D_{NH}| \leq 30$ Hz, one calculates an effective range of *J* mismatch, $J_{CH}^{mis} \leq 0.15$. Inside this range, the three-step filter using $k = 0.73$ yields perfect suppression of the unwanted signals ($I^{sup}/I^{sel} < 0.01$).

The ^1H doublet lines are separated into subspectra using an IPAP type α/β spin-state-selection filter[15] inserted prior to the final INEPT step between time points d and e in the sequence of Figure 2A. Neglecting relaxation effects and the influence of $^1H-^1H$ dipolar coupling, we arrive at the spin evolution during the filter delay $2\tau_a = 1/2J_{CH}$ by

$$2C_yH_y \rightarrow 2C_yH_y \cos(2\pi J_{CH}^{eff}(\tau_a - 2\delta)) + 4C_xH_yH_z \sin(2\pi J_{CH}^{eff}(\tau_a - 2\delta)) \quad (9)$$

The inphase or antiphase ^1H coherence term is selected for detection by setting the filter delay δ to either (I) $\delta = \tau_a/2$ or (II) $\delta = 0$ and adjusting the phase φ_2 of the subsequent 90° ^{13}C pulse. Additional D_{HH}^{met} coupling evolution during the filter

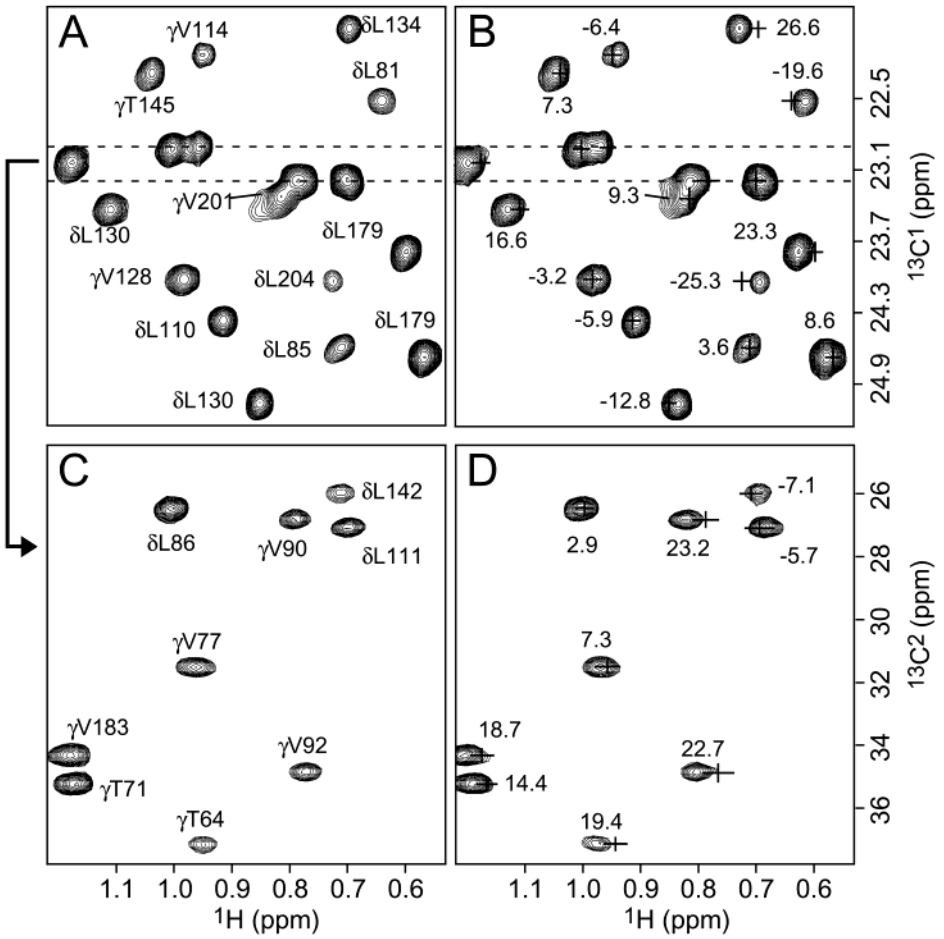

Figure 4. Part of the 2D D_{HH}-CT-HSQC (A) α and (B) β subspectra recorded on the SiR-FP18 phage sample at 30°C and 600 MHz ^1H frequency. The correlation peaks are annotated by the residue number in part A and by the measured D_{HH}^{met}, coupling constant (in Hz) in part B. 2D planes extracted at the methyl $^{13}C^1$ frequency of $\omega_1 = 23.0$ ppm from the 3D D_{HH}-CT-HCC spectrum recorded on the SiR-FP18 phage sample at 30°C and 600 MHz ^1H frequency are shown in (C) α subspectrum and (D) β subspectrum. The resonance frequencies of C^β of threonine are outside the chosen $^{13}C^2$ spectral width (SW) and are detected at a position (ω_C-SW) in spectra C and D.

and the final INEPT delays interconvert ^1H inphase and antiphase coherence. The undesired coherence transfer pathway is suppressed by the π/4-pulse sandwich applied at time point f just before the final detection period. The D_{HH} coupling evolution during the delay $4\tau_a$ results in a signal attenuation of

$$\cos(\pi D_{HH}^{met} 4\tau_a) = \cos\left(\pi \frac{D_{HH}^{met}}{J_{CH}}\right) = \cos(\pi \lambda_1 J_{CH}^{mis}) \approx \cos(2\pi J_{CH}^{mis}) \quad (10)$$

This signal attenuation yields sensitivity losses of 20% for methyl sites with a J mismatch of $J_{CH}^{mis} = 0.10$ and of 40% for methyl sites with $J_{CH}^{mis} = 0.15$. Therefore, the experiment will perform best for moderate molecular alignment conditions. No J-mismatch compensation filter was used for the α/β spin-state selection to avoid an even more significant signal loss during the longer filter delays. For $J_{CH}^{mis} = 0.15$, the residual peak intensity is about 1.4% of the intensity of the selected peak, which will not significantly affect the accuracy of the D_{HH}^{met} measurement.

3D D_{HH}-CT-HCC Method. For larger proteins with an increasing number of overlapping $^{13}C^1-^1H$ correlation peaks, it will be advantageous to measure the D_{HH}^{met} dipolar couplings from a 3D spectrum where the methyl $^{13}C^1-^1H$ correlation peaks are dispersed in the additional $^{13}C^2$ dimension. In the HCC spectrum, the correlation peaks of different amino acid types can be distinguished by their characteristic C^2 frequency. The 3D D_{HH}-CT-HCC pulse sequence of Figure 2B uses the same filter elements for isotopomer selection and α/β spin-state selection as those described for the 2D D_{HH}-CT-HSQC experiment. In the CT-HCC experiment, magnetization is transferred in an "out and back" fashion from the methyl protons via the directly attached C^1 to the C^2 carbon by the following transfer steps

$$H \xrightarrow{J_{CH}^{eff}} C^1(\mathrm{CT} - t_1) \xrightarrow{J_{CC}^{eff}} C^2(\mathrm{CT} - t_2) \xrightarrow{J_{CC}^{eff}} C^1 \xrightarrow{J_{CH}^{eff}} H(t_3) \quad (11)$$

where the active couplings involved in each transfer are indicated above the arrows. As the methyl groups are located at the side chain ends, the ^1H magnetization can be transferred completely to the C^2 carbon if the transfer delays are correctly adjusted and relaxation effects are neglected. The transfer amplitudes are also little affected by the residual dipolar coupling contribution (for $J_{CH}^{mis} = 0.15$, the maximal mismatch of the $^{13}C-^{13}C$ coupling is $J_{CC}^{mis} = 0.24$). C^1 frequency editing and CH_2D spin-state selection are performed during the $^{13}C \rightarrow {}^{13}C$ transfer delay $2\Delta = 1/2J_{CC}$. The t_2 period is also recorded in a CT mode to avoid signal attenuation and line splitting due to J_{CC} coupling evolution. For highly deuterated proteins, only

the $C^1H_2D-C^2D$ labeled methyl side chains (see Figure 3) contribute to the detected signal, as the ^{13}C in a C^2H group will relax rapidly during the CT delay. The CT-HCC experiment benefits from the long transverse relaxation times of both the C^1 and C^2 carbon spins in the $C^1H_2D-C^2D$ fragment, due to the rapid methyl rotation for C^1 and the absence of an efficient relaxation mechanism for C^2.

Extraction of D_{HH}^{met} Values. Addition of the two spectra I and II recorded with the α/β spin-state-selection filter yields the spectrum of the $2H_yH^\beta = H_y + 2H_yH_z$ transition (β subspectrum), whereas subtraction yields the spectrum of the $2H_yH^\alpha = H_y - 2H_yH_z$ transition (α subspectrum). The peak positions in the α and β subspectra are given by $\upsilon^\beta = \upsilon_C + D_{HH}^{met}/2$ and $\upsilon^\alpha = \upsilon_C - D_{HH}^{met}/2$, respectively. The $^1H-^1H$ dipolar coupling is obtained from an accurate measurement of the peak position along the ^1H dimension in the 2D or 3D α/β subspectra as:

$$D_{HH}^{met} = \upsilon^\beta - \upsilon^\alpha \tag{12}$$

Figure 4 demonstrates the quality of the 2D CT-HSQC spectra recorded with the sequence of Figure 2A on the SiR-FP18 phage sample. A small part of the α and β subspectra is displayed in Figure 4A and B, respectively. Peaks which are sufficiently well resolved are annotated in part A by the residue type and number, and in part B by the measured D_{HH}^{met} coupling constant. For SiR-FP18, 65 methyl D_{HH}^{met} constants could be accurately measured using the 2D approach. Most overlapping correlation peaks are resolved in the 3D CT-HCC spectra, as illustrated for 2D planes extracted at a methyl $^{13}C^1$ frequency of $\omega_1 =$ 23.0 ppm in Figure 4C (α subspectrum) and D (β subspectrum). Note that despite the fact that only about 10% of the molecules contribute to the signal in the 3D spectrum because of the $C^1H_2D-C^2D$ selection, a high signal-to-noise ratio is obtained for SiR-FP18 in a reasonable experimental time (70 h) on a 600 MHz NMR spectrometer. The sensitivity of the experiment is mainly limited by the fact that only a small number of molecules contribute to the detected signal, and not by relaxation-induced signal loss during the coherence transfer and CT frequency editing delays. Simulations shown in Figure S3 of the Supporting Information show that the sensitivity of the experiment drops by about 30% and 50% when increasing the rotational correlation time of the molecule from 10 ns to 20 ns and 30 ns, respectively. This loss can be compensated by the use of higher field magnets or cryoprobe technology. We therefore expect that the experiment will be applicable to proteins of considerably higher molecular weight than SiR-FP18.

Side Chain Orientation from Methyl D_{HH}. Side chain structure refinement in proteins is generally based on a set of $^1H-^1H$ NOE. For larger proteins, the sensitivity of NOESY type experiments decreases and the resonance frequencies become increasingly degenerate. It is thus often difficult to detect and unambiguously assign sufficient NOE peaks for defining a high-resolution structure of the protein core. Methyl RDCs add an additional independent source of NMR constraint for side chain conformation. As shown earlier, they can be accurately measured on highly deuterated protein samples, which makes this approach particularly attractive for the study of large proteins. Out of the 167 residues of SiR-FP18, 70 (42%) have methyl containing side chains (Ala, Ile, Leu, Met, Thr, and Val). Most of them

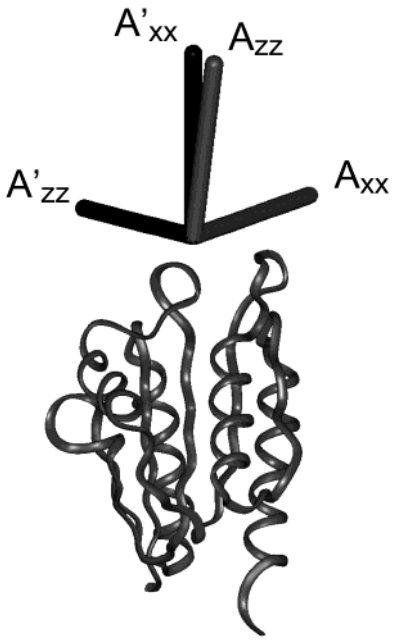

Figure 5. Orientation of the molecular alignment tensors in the phage (black) and alcohol (gray) environment. The backbone representation of SiR-FP18 at the bottom shows the orientation of the molecule with respect to the two tensors.

are likely to be in the hydrophopic core of the protein in analogy to homologous structures. The measured D_{HH}^{met} can be directly exploited as constraints for the C^1-C^2 bond vector orientations with respect to the molecular alignment tensor using eq 7 by inserting a methyl RDC penalty function into a standard molecular-dynamics-based structure calculation protocol. The molecular alignment tensors can be obtained from a set of backbone RDCs measured on the same partially aligned protein sample. In favorable cases, this can be achieved using *de novo* structure calculations,[8] although in the present case the tensors can be calibrated directly in comparison with a close structural homology model.[17] The large number and orientational distribution of the backbone vectors for which RDC can be measured allow accurate determination of the tensor parameters. For SiR-FP18, the axial and rhombic components of the molecular alignment tensors are $A_a = -16.9 \times 10^{-4}$ and $A_r = -11.3 \times 10^{-4}$ for the phage sample and $A_a = -18.2 \times 10^{-4}$ and $A_r = -10.5 \times 10^{-4}$ for the alcohol sample. The relative orientations of the two tensors is plotted in Figure 5. Despite the similar asymmetries and rhombicities of the two tensors, the different orientations ensure that complementary structural information is obtained from the two sets of D_{HH}^{met} values.

In practice, backbone and side chain RDC measurements are often not performed at the same time. This may result in slightly altered tensor characteristics for the two measurements because of aging of the sample. These changes can be taken into account by remeasuring a set of backbone D_{NH} couplings and comparing them with the previously obtained values. For the present study, the methyl RDC measurements were performed several months after sample preparation and recording of the backbone RDC experiments. The linear correlation of the two data sets indicates that the tensor orientations for the phage and alcohol samples (Figure S1A and B of the Supporting Information) remain unchanged. The differences in the principal axis values can be taken into account by the scaling factor λ_{scale} in eq 7, which

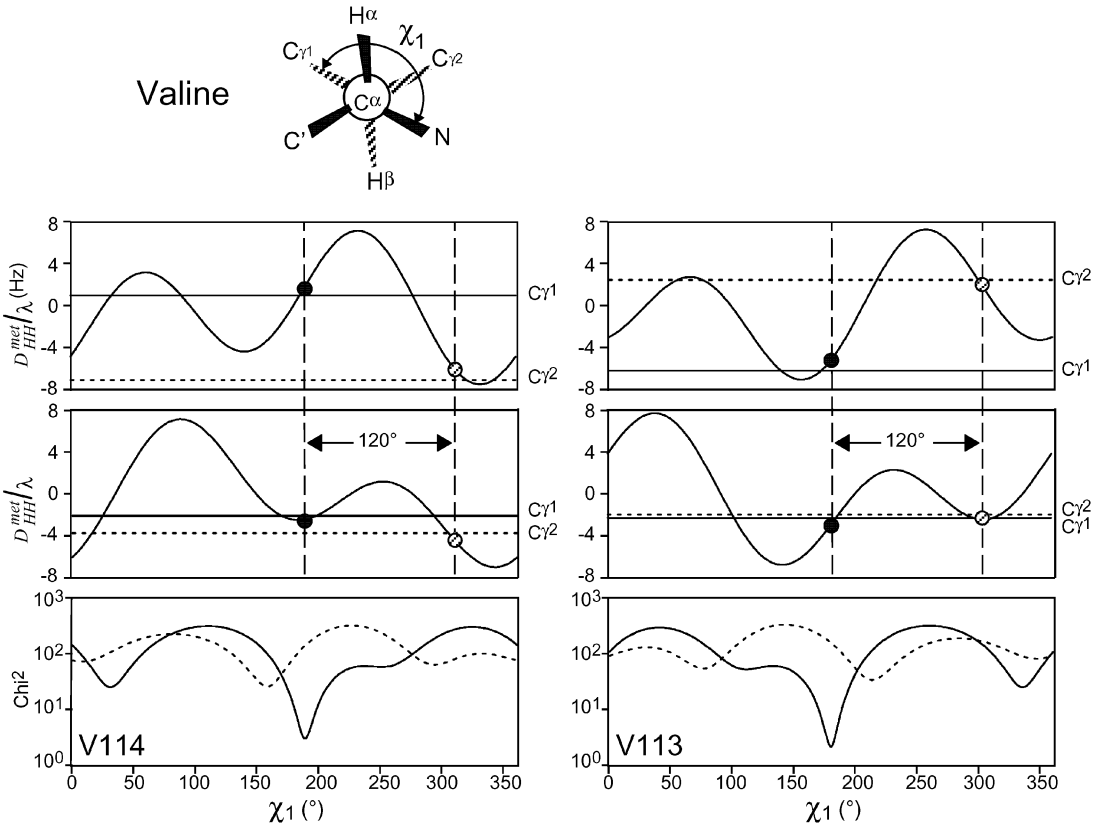

Figure 6. $D_{HH}^{met}(\chi_1)$ calculated for the two valine residues Val113 and Val114 using eq 7. The upper curve corresponds to the calculation for the phage sample; the middle curve corresponds to the calculation for the alcohol sample. The orientation of the $C^{\alpha}-C^{\beta}$ vector with respect to the molecular alignment frame was extracted from the RDC-refined model structure of SiR-FP18.[17] The lower curve shows the error function $Chi^2(\chi_1)$ as defined by eq 13 calculated for the two stereospecific methyl assignments. The experimental error was set to $\sigma = 1$ Hz for all measurements. The experimentally observed D_{HH}^{met} values are indicated by solid (methyl 1) and dashed lines (methyl 2).

can be estimated from the slope of the correlation plots in Figure S1. The validity of this approach is independently confirmed by the D_{HH}^{met} couplings measured for alanine residues, which depend on the $C^{\alpha}-C^{\beta}$ bond vector orientation in the backbone-refined structure of SiR-FP18. The measured couplings correlate well with the back-calculated values using eq 7 with $r_{cc}^{eff} = 1.52$ Å, $\lambda_1 = 2.28$, $\lambda_2 = -3.17$, and λ_{scale} as extracted from the slope of the D_{NH} correlation plots (Figure S1C and D). This result is also in agreement with a slight deviation from ideal tetrahedral geometry, as recently shown by Bax and co-workers[27] for CH_3 methyl groups. The replacement of a proton by a deuteron in the methyl does not seem to significantly alter the methyl geometry.

χ_1 Torsion Angles and Stereospecific Assignment of Methyl Groups in Valine Side Chains. Alternatively to their general use as constraints in a molecular-dynamics-based structure calculation protocol, the methyl RDCs of valine residues can also be used for direct determination of χ_1 torsion angles, which can then be reintroduced into the structure refinement procedure. On the basis of the refined backbone structure, D_{HH}^{met} values can be computed as a function of χ_1 for each residue and alignment medium. The tool developed to calculate these values is compatible with the MODULE[18] output format and is available from the authors. It is useful to reiterate the importance of measuring RDCs in two differently aligning media to raise the orientational degeneracy of a single vector (or methyl axis) relative to the common alignment tensor. For valine side chains, the two $C^{\beta}-C^{\gamma}$ vectors constitute a planar motif, whose orientation is defined with a 2-fold degeneracy in the presence of two alignment media. In the absence of noise, the native orientation can be distinguished from the mirror image on the basis of covalent considerations at the C^{β} tetrahedral center. While the correct conformation will respect the expected 109.5° covalent angles, the image will have $C^{\alpha}-C^{\beta}-C^{\gamma}$ angles of 70.5°. The algorithm therefore supposes a tetrahedral geometry, effectively eliminating the mirror-image conformation. An additional constraint concerning the unknown stereospecific assignment requires that both possible assignments are tested.

Figure 6 shows D_{HH}^{met} values plotted as a function of the torsion angle χ_1 for two representative examples of valine side chains. A different dependence on the χ_1 angle is obtained for the phage and alcohol samples because of the different alignment characteristics (see Figure 5). The experimentally obtained values are indicated by solid and dashed lines for the two methyl groups. The best-fit value of χ_1 is obtained by minimizing the target function:

$$\mathrm{Chi}^2 = \sum_i \sum_k \frac{({}^{exp}D_{HH}^{met}/\lambda - {}^{calc}D_{HH}^{met}(\chi_1)/\lambda)_{i,k}^2}{\sigma_{i,k}^2} \qquad (13)$$

where ${}^{calc}D_{HH}^{met}(\chi_1)$ is given by eq 7, ${}^{exp}D_{HH}^{met}$ is the experimental RDC value for methyl group k and alignment medium i, and $\sigma_{i,k}$ is the experimental error of the measured coupling value. $Chi^2(\chi_1)$ is also plotted in Figure 6. The two different curves

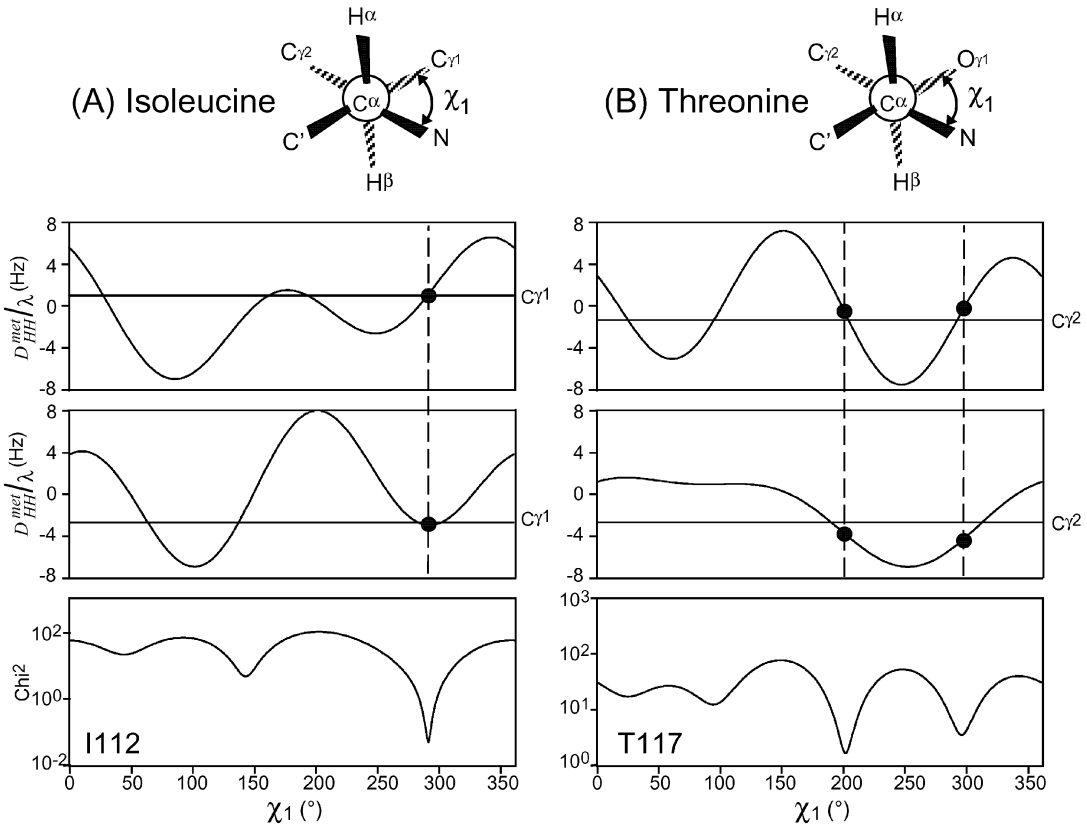

Figure 7. $D_{HH}^{met}(\chi_1)$ and $Chi^2(\chi_1)$ plots for an (A) isoleucine and (B) threonine side chain. The experimentally observed D_{HH}^{met} values are indicated by solid lines.

Table 1. χ_1 Torsion Angles and Stereospecific Assignments of Prochiral Methyl Groups in Valine Residues of SiR-FP18

residue	χ_1[a] [deg]	Chi[2b]	$C^{\gamma 1}$ ($H^{\gamma 1}$) [ppm]	$C^{\gamma 2}$ ($H^{\gamma 2}$) [ppm]
Val77	25	0.7	23.1 (0.97)	20.8 (0.53)
	178	2.3	20.8 (0.53)	23.1 (0.97)
Val92	200	1.6	23.4 (0.78)	19.8 (0.92)
Val113	179	1.9	19.5 (0.19)	19.8 (0.54)
Val114	188	2.8	22.1 (0.94)	20.8 (0.84)
Val128	160	2.9	20.8 (0.89)	24.2 (0.97)
	175	3.3	24.2 (0.97)	20.8 (0.89)
Val183	174	5.5	21.6 (0.74)	22.9 (1.18)
Val187[c]	1	7.1	22.2 (1.27)	21.9 (1.18)
Val200	152	2.6	22.8 (0.30)	22.2 (−0.24)
	229	3.0		
Val201	174	2.9	21.3 (0.77)	23.4 (0.82)

[a] Best fit value of dihedral angle χ_1. [b] Minimum of error function defined in eq 13 at best fit χ_1 value. [c] Val187 is in a loop region which is ill-defined in the RDC-refined model structure of SiR-FP18.[17]

(solid and dashed lines) correspond to a different stereospecific assignment of the two methyl groups. The curves in Figure 6 show that the two valine side chains at positions 113 and 114 adopt a trans configuration ($\chi_1 \approx 180°$). Table 1 summarizes the best-fit χ_1 values and stereospecific assignments for the nine valines for which D_{HH}^{met} data were obtained. The methyl RDC data of Val217 could not be analyzed as this residue is not present in the C-terminal-truncated NMR-refined homology model of SiR-FP18.[17] For five valine side chains (Val92, Val113, Val114, Val183, and Val201) a unique solution is found with a χ_1 angle close to 180°. For Val77 and Val128, a similar minimum of the error function $Chi^2(\chi_1)$ is obtained for both stereospecific assignments. In the case of Val77, one solution corresponds to a trans configuration ($\chi_1 = 178°$), whereas the other one is an eclipsed conformation ($\chi_1 = 25°$) which is rather unlikely for valine side chains. For Val 128 the two solutions are only 15° apart ($\chi_1 = 160°$ or 175°), indicating that the side chain is probably in a trans configuration. While the stereospecific assignment is well defined for Val200, the $Chi^2(\chi_1)$ function has two similar minima at $\chi_1 = 152°$ and $\chi_1 = 229°$. It is not possible to discriminate between the two solutions. The last example is Val187, for which a well-defined but rather unlikely minimum of the $Chi^2(\chi_1)$ function is obtained at an angle $\chi_1 = 1°$. Val187 is situated in a loop region of the protein connecting the strand β_5 with the C-terminal helix α_4. The backbone of this loop is only poorly defined in the RDC-refined model structure. An erroneous orientation of the $C^{\alpha}-C^{\beta}$ vector with respect to the molecular frame will change the $Chi^2(\chi_1)$ curves and may result in a wrong χ_1 value for this residue. In summary, seven out of nine valine side chains could be identified to be in a trans configuration, whereas for one residue two equally probable solutions are found, and Val187 has been removed from the analysis because of the ill-defined backbone conformation in this region of the molecule. Comparable results for the stereospecific methyl assignment and χ_1 torsion angles are obtained from a conventional analysis based on $^1H-^1H$ NOE and $^3J_{\alpha\beta}$ scalar coupling constants measured on a [U−^{13}C, U−^{15}N, ^{1}H] labeled sample of SiR-FP18. The results are summarized in Table S2 of the Supporting Information. We note that the conventional approach fails for overlapping ^{1}H frequencies of the two methyls (for NOE measurements) or overlapping $H^{\alpha}-C^{\alpha}$ correlation peaks (for $^3J_{\alpha\beta}$ measurements).

χ_1 Torsion Angles in Isoleucine and Threonine Side Chains. A similar analysis, as shown earlier for valine side

chains, is also possible for isoleucine and threonine residues. In contrast with valine, the χ_1 angle in isoleucine and threonine is only defined by the D_{HH}^{met} values measured for one methyl (instead of two) in the different alignment media. The orientation of the second methyl group of isoleucine ($C_{\delta 1}$) is also dependent on the χ_2 torsion angle. In favorable cases, the RDC data are sufficient to define a single minimum. Such an example is given by Ile112 shown in Figure 7A, where a single well-defined minimum of the $Chi^2(\chi_1)$ function can be distinguished corresponding to a staggered conformation with $\chi_1 = -71°$. In most cases, however, the methyl RDC data are not sufficient to unambiguously define the rotameric state of these side chains. This is illustrated for Thr117 in Figure 7B, where at least two possible solutions are obtained for the χ_1 angle. The remaining ambiguities may be solved by the measurement of D_{HH}^{met} under additional alignment conditions or by adding complementary NMR data such as RDCs of other side chain vectors or $^1H-^1H$ NOE.

Conclusions and Perspectives

The use of highly deuterated samples is mandatory for structural NMR studies of high molecular weight systems. In combination with TROSY type experiments, the use of high-level deuteration allows sequential assignment of the backbone resonances and identification of secondary structural elements. The fold of the protein backbone can be determined from a set of measured backbone RDCs and amide proton NOE. The lack of side chain protons, however, makes it difficult to obtain a high-resolution NMR structure of the protein core using standard $^1H-^1H$ NOE based methods. Selective methyl protonation has been proposed in the past[28] to partially overcome this problem. Here, we have shown that methyl RDCs can be measured accurately on a highly deuterated protein sample. The methyl ^1H and ^{13}C resonances were assigned using ^{13}C-TOCSY type experiments performed on the same protein sample. Methyl RDCs provide valuable information on side chain conformation. In particular, if two different alignment tensors are available D_{HH}^{met} measurements can be used to determine χ_1 torsion angles in valine side chains. In addition, stereospecific assignment of the prochiral methyl groups is obtained.

Methyl RDCs are potentially very powerful tools for *de novo* structure determination before overall fold is known, as they provide important complementary structural information to NOE data measured on a selectively protonated sample. Backbone couplings measured in motifs of secondary structure whose local conformation is known, or can be estimated (for example an α-helix), allow the precise determination of the alignment tensors, irrespective of the fold of the molecule. The use of sparse methyl−methyl or methyl−amide proton NOE data to position these oriented structural elements should be significantly improved because of the increased structural precision of methyl containing side chains described here.

Methyl RDCs may also become interesting in the context of NMR studies of intermolecular interactions. As small changes in side chain orientation will result in a measurable change in the residual dipolar coupling, methyl RDCs can be used as efficient probes of structural changes which may occur, for example, upon ligand binding, without undertaking a complete structure determination.

Acknowledgment. This work was supported by the Commissariat à l'Energie Atomique and the Centre National de la Recherche Scientifique. N.S. acknowledges the receipt of a Ph.D. fellowship from the French ministry of research and technology.

Supporting Information Available: Two tables containing $^1H-^1H$ methyl RDCs and $^1H-^1H$ NOE and $^3J_{\alpha\beta}$ coupling data measured for SiR-FP18. Correlation plots of backbone N−H RDCs measured directly after sample preparation and several months later and correlation plots of measured versus back-calculated methyl RDCs for alanine residues. Examples of 2D planes extracted from amide-detected ^{13}C-TOCSY experiments recorded on a 77% deuterated SiR-FP18 sample for assignment of the methyl ^1H and ^{13}C resonances. Simulations of relaxation-induced signal loss during the 3D D_{HH}-CT-HCC experiment as a function of the molecular tumbling correlation time. This material is available free of charge via the Internet at http://pubs.acs.org.

JA020888M

(28) Gardner, K. H.; Kay, L. E. *Annu. Rev. Biophys. Biomol. Struct.* **1998**, *27*, 357−406.